Predictive value of ^{18}F-fluorodeoxyglucose positron emission tomography - computed tomography compared to postoperative pathological findings for patients with non-small-cell lung cancer

JIE XUE[1,2], JINSONG ZHENG[3], HONGBO GUO[4], XIAOHUI WANG[3] and ANQIN HAN[5,6]

[1]Department of Oncology, The Affiliated Hospital of Shandong Academy of Medical Sciences, Jinan, Shandong 250031; [2]School of Medicine and Life Sciences, University of Jinan-Shandong Academy of Medical Sciences, Jinan, Shandong 250022; Departments of [3]Nuclear Medicine, [4]Thoracic Surgery and [5]Radiation Oncology and [6]Key Laboratory of Radiation Oncology of Shandong Province, Shandong Cancer Hospital, Jinan, Shandong 250117, P.R. China

Received March 6, 2014; Accepted August 12, 2014

DOI: 10.3892/mco.2014.408

Abstract. This study was conducted to investigate the predictive value of ^{18}F-fluorodeoxyglucose positron emission tomography-computed tomography (^{18}F-FDG PET-CT) in patients with non-small-cell lung cancer (NSCLC), compared to that of postoperative pathological findings, for T and N staging and the associations of the metabolic parameters of the primary tumor with histological type and differentiation. The preoperative contrast-enhanced CT and ^{18}F-FDG PET-CT and postoperative pathological findings of 112 NSCLC patients treated with lobectomy or pneumonectomy combined with systematic mediastinal lymphadenectomy were retrospectively reviewed. Compared to the postoperative pathological findings, the effect of contrast-enhanced CT and ^{18}F-FDG PET-CT on T and N staging were evaluated. The metabolic tumor volume (MTV) and maximum standardized uptake value (SUVmax) of the primary tumor were measured. The associations between these metabolic parameters and histological type and differentiation were also evaluated. The differences in the accuracy in overall staging and T staging between PET-CT and contrast-enhanced CT were significant (91.1 vs. 69.6%, P=0.000; and 92.9 vs. 76.8%, P=0.000, respectively). The sensitivity, specificity, positive predictive value, negative predictive value and accuracy of regional lymph node metastasis detection were 91.7, 93.0, 86.5, 95.8 and 92.6%, respectively, with PET-CT; and 71.3, 77.2, 60.6, 84.5 and 75.2%, respectively, with contrast-enhanced CT. The SUVmax (7.29±1.83 vs. 5.91±1.65, t=4.15, P=0.000) and MTV (48.20±2 2.47 vs. 30.21±19.72 cm^3, t=4.48, P=0.000) were significantly higher for squamous cell carcinoma (SCC) compared to those for adenocarcinoma (AC). There was a positive correlation between the MTV and SUVmax of the primary tumor (Pearson's r=0.838, P=0.000). Significant differences were observed among differentiation subgroups in the SUVmax and MTV of the primary tumor for both SCC and AC. In conclusion, compared to the postoperative pathological findings, the predictive value of ^{18}F-FDG PET-CT for T and N staging in NSCLC was higher compared to that of contrast-enhanced CT. The FDG uptake of the primary tumor was associated with histological type and differentiation and the difference was statistically significant. Therefore, the SUVmax and MTV of the primary tumor may be valuable indices to partly predict the histological type and grade of differentiation of NSCLC.

Correspondence to: Dr Anqin Han, Department of Radiation Oncology, Shandong Cancer Hospital, 440 Jiyan Road, Jinan, Shandong 250117, P.R. China
E-mail: dochaq@126.com

Key words: positron emission tomography, computed tomography, non-small-cell lung cancer, staging, standardized uptake value, metabolic tumor volume

Introduction

Histological classification and staging are crucial for treatment selection in non-small-cell lung cancer (NSCLC). Squamous cell carcinoma (SCC) and adenocarcinoma (AC) are the two most common types of NSCLC. Due to their dependence on tumor-associated structural changes, conventional imaging modalities are inaccurate in the assessment of lymph node metastases (1) and tumor size when combined with obstructive pneumonia and atelectasis in NSCLC. One of these modalities, contrast-enhanced computed tomography (CT), has been widely used for preoperative evaluation. However, ^{18}F-fluorodeoxyglucose positron emission tomography (^{18}F-FDG PET) may be more sensitive compared to CT, as the alterations in tissue metabolism measured by PET generally precede anatomical changes. Coregistration of PET and CT by using a combined PET-CT system was found to be of additional value for image interpretation. The purpose of the present study was to investigate the predictive value of ^{18}F-FDG PET-CT for patients with NSCLC, compared to that of postoperative pathological findings, for T and N staging and

the associations of primary tumor metabolic parameters with histological type and differentiation.

Patients and methods

Patients. We retrospectively reviewed all patients with a confirmed diagnosis of NSCLC by postoperative pathological findings in Shandong Cancer Hospital between May, 2003 and November, 2011. The patients were treated with lobectomy or pneumonectomy combined with systematic mediastinal lymphadenectomy and complete data on preoperative contrast-enhanced CT of the chest, ^{18}F-FDG PET-CT and postoperative pathological findings were available. Following the standard preoperative staging procedures, including physical examination, laboratory tests, ultrasound of the neck and abdomen and recommendation for FDG PET-CT staging, all the patients were found to be without distant metastasis and suitable for operative treatment. Patients who had received prior anticancer treatment were excluded, as were patients with diabetes mellitus and coexistent malignant conditions. Surgical specimens that were intact and histologically confirmed as AC or SCC were further examined. Due to their lower incidence, other histological subtypes, such as large-cell carcinoma, were eliminated to homogenize the study.

The study protocol was approved by the Institutional Review Board of Shandong Cancer Hospital. Informed consent was waived due to the retrospective design of the study. In this retrospective study, data from 112 patients meeting the eligibility criteria were evaluated. The characteristics of the patients are summarized in Table I.

Table I. Patient characteristics.

Characteristics	Cases, no. (%) (n=112)
Age (years)	
<60	96 (85.7)
≥60	16 (14.3)
Gender	
Male	78 (69.6)
Female	34 (30.4)
Tumor side	
Right	68 (60.7)
Left	44 (39.3)
Primary tumor location	
Upper lobe[a]	72 (64.3)
Lower lobe	40 (35.7)
Surgical procedure	
Lobectomy	92 (82.1)
Bilobectomy	14 (12.5)
Pneumonectomy	6 (5.4)
Histological type	
Squamous cell carcinoma	59 (52.7)
Adenocarcinoma	53 (47.3)
Tumor differentiation	
High	43 (38.4)
Moderate	38 (33.9)
Poor	31 (27.7)

[a]Including middle lobe tumors on the right side.

CT technique. All the patients included in this study underwent preoperative multidetector CT with a 16-detector row CT scanner (Sensation 16; Siemens, Erlangen, Germany) according to an established protocol. Each patient was fasted for 6 h prior to undergoing contrast-enhanced CT in the supine position with the arms crossed overhead. Intravenous administration of 70 ml of the iodinated contrast material iopromide (Ultravist; Bayer Schering Pharma, Berlin, Germany), containing 300 mg iodine/ml, via power injection at a rate of 2.5 ml/sec, was performed. The scan was initiated at 25-30 sec after injection, at 140 kV and 230 mA with 0.75-7.0 mm section collimation, a pitch of 1.0-1.5 and 3.0 mm of reconstruction thickness.

^{18}F-FDG PET-CT. ^{18}F-FDG PET-CT scans were obtained with an integrated PET-CT system (Discovery LS; GE Healthcare, Piscataway, NJ, USA). All the patients were fasted for at least 6 h and rested for 15 min, then injested 500 ml of water prior to the injection of 400 MBq of the radioactive tracer (^{18}F-FDG). The serum glucose levels were measured to ensure that they were <6.6 mmol/l. The patients received no urinary bladder catheterization, no oral muscle relaxants and no CT contrast agents. For ~60 min (range, 50-65 min) following ^{18}F-FDG injection, the patients were reclined in a quiet room with minimal muscular activity. The patients were then immobilized using a custom immobilization cradle in the supine position with the arms placed on the sides. The PET-CT system was used for 4-slice helical CT acquisition, followed by a full-ring dedicated PET scan of the same axial range. The CT component was operated with an X-ray tube voltage peak of 120 kV, 90 mA, a 6:1 pitch, a slice thickness of 5 mm and a rotational speed of 0.8 sec/rotation. PET scans were obtained from the level of the middle skull to that of the proximal thigh for 4 min/field of view, each covering 14.5 cm, at an axial sampling thickness of 4.25 mm/slice. Both PET and CT scans were obtained during normal tidal breathing. The PET images were reconstructed with CT-derived attenuation correction using ordered-subset expectation maximization software. The attenuation-corrected PET images, CT images and fused PET-CT images were available for review in the axial, coronal and sagittal planes and a cine display of maximum intensity projections of the PET data, using the manufacturer's review station (Xeleris; GE Healthcare). The local delayed scanning was performed at ~120 min (range, 110-140 min) following the ^{18}F-FDG injection when it was difficult to make a differential diagnosis between benign and malignant lesions (dual-time-point imaging). The acquisition parameters for the dual-time-point scan were identical.

Analysis on imaging. Contrast-enhanced CT and PET-CT images were assessed by two reader teams that consisted of different physicians. Each of the evaluating teams had the same information on the patient's clinical history. The two

evaluating physician teams were blinded to the results of the other imaging examinations and the postoperative pathological findings.

The contrast-enhanced CT findings of each patient were reviewed by 3 experienced radiologists. The CT images were viewed in coronal, axial and sagittal sections, applying an appropriate window width and window level. Lymph nodes (LNs) with a short-axis diameter >1 cm were defined as malignant. Furthermore, the presence of a central unenhancing area suggesting central necrosis was considered a sign of malignancy, regardless of the nodal size (1).

On the Xeleris station, CT, PET and fused PET-CT images were simultaneously opened and reviewed by 3 experienced nuclear medicine physicians and radiologists. The PET-CT images were reviewed and interpreted by consensus, comparing and analyzing the PET and CT images side by side, using visual observation and semi-quantitative analysis. For visual interpretation, the findings were considered to be positive for lesions with asymmetrically increased FDG accumulation; they were also considered positive when the maximum standard uptake value (SUVmax) of the region of interest (ROI) exceeded 2.5. For dual-time-point imaging, the SUVmax of the initial scan was $SUVmax_{initial}$ and the SUVmax of the delayed scan was $SUVmax_{delayed}$. The retention index (RI) represented the percent change of ^{18}F-FDG uptake and was calculated as follows: $RI = \Delta SUVmax/SUVmax_{initial}$ x100%, $\Delta SUVmax = SUVmax_{delayed}-SUVmax_{initial}$ and RI >10% was considered as a criterion for the diagnosis of malignancy, a threshold that has been widely used in previous studies (2-5). In this study, we limited metabolic tumor volume (MTV) by a fixed SUV of 2.5, a threshold that has been widely used for diagnosis in previous studies (6-8). All the measurements were performed on the combined PET-CT images. The MTV was delineated on the PET images in transaction slice by slice automatically with the SUV 2.5 isocontour. The tumor volume was then automatically calculated with the fusion software by adding up the transverse delineations slice by slice to a total volume. Of note, the cavity or non-avid area in tumors, when present, was excluded as part of the MTV. Furthermore, the SUVmax within the MTV was also automatically calculated.

Surgical procedures. Lobectomy or pneumonectomy combined with systematic mediastinal lymphadenectomy was successfully performed by experienced thoracic surgeons within 1 week after contrast-enhanced CT and PET-CT imaging, including 92 cases of lobectomy and 14 cases of bilobular lobectomy, as well as 6 cases of pneumonectomy. According to descriptions by Naruke *et al* (9), Martini and Flehinger (10) and Izbicki *et al* (11), systematic mediastinal lymphadenectomy was defined as removal of levels 2-4, 7-9 and 10-12 during a right thoracotomy and levels 2-9 and 10-12 during a left thoracotomy.

T and N staging and standard of reference. According to the newly revised American Joint Comittee on Cancer TNM system for the classification of lung cancer (12,13), T and N staging was performed by a tumor board consisting of 3 radiation oncologists, who were not involved in imaging evaluation in this study. T and N staging by the tumor board was based on contrast-enhanced CT (CT staging), PET-CT (PET-CT staging) and postoperative pathological findings (standard of reference). Patients in whom the T and N stages were overestimated were characterized as overstaged, whereas those with underestimated T and N stages were characterized as understaged.

Statistical analysis. The results of the imaging modalities were compared with a reference standard provided by pathological examination of each nodal group. PET-CT positive results were defined as true positive (TP) when confirmed by histopathological examination as lymph node metastases and as false positive (FP) when the histopathological examination of the resected nodal group revealed no evidence of metastasis. A site characterized as a negative area was defined as true negative (TN) when the histopathological examination of the resected nodal group revealed no metastatic disease and as false negative (FN) when there was subsequent histopathological proof of lymph node metastasis. The formulae for calculating the diagnostic efficacy of contrast-enhanced CT and PET-CT were as follows: sensitivity = TP/(TP+FN), specificity = TN/(TN+FP), positive predictive value = TP/(TP+FP), negative predictive value = TN/(TN+FN) and accuracy = (TP+TN)/(TP+FP+TN+FN). Differences between the two imaging modalities were assessed using the McNemar test with Bonferroni adjustment. Comparisons of different continuous parameters (SUVmax and MTV) between different groups were performed with the independent samples t-test or ANOVA. Pearson's correlation was used to estimate the association between MTV and SUVmax. $P<0.05$ was considered to indicate a statistically significant difference. The SPSS statistical software, version 17.0 (SPSS, Inc., Chicago,. IL, USA) was used for the analysis.

Results

Overall staging. Among the 112 patients, PET-CT staging was consistent with pathological staging in 102 cases. The accuracy of overall staging was 91.1%, while that of contrast-enhanced CT staging was 69.6%. The difference in the accuracy of overall staging between contrast-enhanced CT and PET-CT was statistically significant (P=0.000).

T staging. T staging was accurately determined in 104 of the 112 patients (92.9%) with PET-CT (overstaging in 6 and understaging in 2 cases). CT correctly assessed 86 cases (76.8%) (overstaging in 18 and understaging in 5 cases). The difference in the accuracy of T staging between contrast-enhanced CT and PET-CT was statistically significant (P=0.001).

The overall staging and T staging by contrast-enhanced CT, FDG PET-CT and postoperative pathological findings are shown in Table II.

N staging. A total of 812 regional LNs were resected from all the patients and 266 were confirmed to be metastatic by postoperative pathological examination. A total of 282 regional LNs were identified as metastatic by PET-CT, including 244 TP and 38 FP. The sensitivity, specificity, positive predictive value, negative predictive value and accuracy of regional lymph node metastasis detection were 91.7, 93.0, 86.5, 95.8 and 92.6%, respectively, with PET-CT; and 71.3, 77.2, 60.6, 84.5 and 75.2%, respectively, with contrast-enhanced CT

Table II. Comparison of staging results by different imaging modalities and postoperative pathological findings.

A, Overall staging by contrast-enhanced CT, FDG PET-CT and postoperative pathological findings

	Results, no. of cases (n=112)		
Stages	Contrast-enhanced CT	FDG PET-CT	Postoperative pathological findings
Ia	15	12	12
Ib	16	15	13
IIA	28	25	22
IIB	33	26	28
IIIA	20	34	37

B, True positive and false negative results in overall staging by contrast-enhanced CT and FDG PET-CT

	FDG PET-CT		
Contrast-enhanced CT	True (+)	False (-)	Total
True (+)	75	3	78
False (-)	27	7	34
Total	102	10	112

C, True positive and false negative results in T staging by contrast-enhanced CT and FDG PET-CT

	FDG PET-CT		
Contrast-enhanced CT	True (+)	False (-)	Total
True (+)	86	3	89
False (-)	18	5	23
Total	104	8	112

Patient-based diagnostic results of interpretations by contrast-enhanced CT, FDG PET-CT, postoperative pathological findings. FDG, fluorodeoxyglucose; PET-CT, positron emission tomography-computed tomography.

(Table III). The difference in the accuracy of N staging between contrast-enhanced CT and PET-CT was statistically significant (P=0.000).

Metabolic parameters. The present study demonstrated the average values for SUVmax (7.28±1.84 vs. 5.91±1.65, t=4.13, P=0.000) and MTV (48.20±22.47 cm^3 vs. 30.21±19.72 cm^3, t=4.48, P=0.000) were significantly higher for SCC compared to AC. There was a positive correlation between the MTV and SUVmax of the primary tumor (Pearson's r=0.838, P=0.000) (Fig. 1). Significant differences were observed among different differentiation subgroups in the SUVmax and MTV of the primary tumor for both SCC and AC (Table IV).

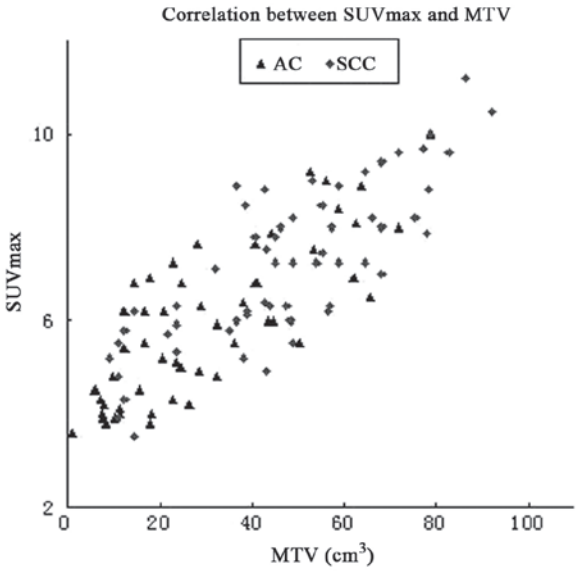

Figure 1. Correlation between maximum standardized uptake value (SUVmax) and metabolic tumor volume (MTV) in the 112 NSCLC patients (Pearson's r=0.838, P=0.000). AC, adenocarcinoma; SCC, squamous cell carcinoma.

Discussion

Our results demonstrated that ^{18}F-FDG PET-CT was superior to contrast-enhanced CT, which has been widely used for clinical staging, for T and N staging in NSCLC patients.

As regards T staging, the difference in the accuracy of T staging between contrast-enhanced CT and PET-CT was

Table III. Results of lymph node metastasis detection with different imaging modalities.

	No. of lymph nodes (n=812)				Value (%)				
Imaging modality	TP	FP	TN	FN	Sen	Spe	PPV	NPV	Acc
Contrast-enhanced CT	189	124	422	77	71.3	77.2	60.6	84.5	75.2
FDG PET-CT	244	38	508	22	91.7	93.0	86.5	95.8	92.6

TP, true positive; FP, false positive; TN, true negative; FN, false negative; Sen, sensitivity; Spe, specificity; PPV, positive predictive value; NPV, negative predictive value; Acc, accuracy; PET-CT, positron emission tomography-computed tomography; FDG, fluorodeoxyglucose.

Table IV. MTV and SUVmax by differentiation and histological subgroup (mean ± SD).

	SUVmax			MTV (cm^3)		
Group	All	SCC	AC	All	SCC	AC
1[a]	5.29±1.10	5.75±1.06	4.80±1.00	23.57±15.97	31.45±17.17	14.52±7.83
2[b]	6.56±1.37	7.27±1.00	5.81±1.19	39.36±16.51	49.04±14.01	30.64±13.65
3[c]	8.59±1.56	9.27±1.29	7.79±1.42	62.43±18.72	68.74±17.81	53.69±16.86
P-value	<0.05	<0.05	<0.05	<0.05	<0.05	<0.05

[a]Well-differentiated subgroup. [b]Moderately-differentiated subgroup. [c]Poorly-differentiated subgroup. SUVmax, maximum standardized uptake value; MTV, metabolic tumor volume; SD, standard deviation; SCC, squamous cell carcinoma; AC, adenocarcinoma.

found to be statistically significant (P=0.000). In a number of NSCLC cases, lesions were identified on CT, including tumor, obstructive pneumonia and atelectasis. However, due to limitations inherent to morphological imaging, CT is frequently compromised by its inability to differentiate viable tumor from adjacent structures, e.g., obstructive pneumonia, atelectasis, chest wall (including superior sulcus tumors), diaphragm, mediastinal pleura and parietal pericardium. FDG PET may be successfully used to identify the metabolic characteristics of the lesions, which are equivocal or even not identified by CT in the majority of the cases.

As regards N staging, FDG PET-CT was also found to be superior to contrast-enhanced CT in the detection and characterization of mediastinal and hilar lymph node metastases. In the present study, the sensitivity, specificity, positive predictive value, negative predictive value and accuracy of regional lymph node metastasis detection were 91.7, 93.0, 86.5, 95.8 and 92.6%, respectively, with PET-CT; and 71.3, 77.2, 60.6, 84.5 and 75.2%, respectively, with contrast-enhanced CT. For PET-CT imaging, FN interpretations of 22 mediastinal and hilar lymph node metastases were primarily attributable to intense tracer accumulation by the primary tumor, limited resolution and ill-defined anatomic boundaries due to respiratory movement or limited microscopic invasion of the LNs; the FP results of 38 regional lymph node metastases were due to reactive lymphadenitis, particularly in patients with obstructive pneumonia, atelectasis and chronic pulmonary disease. The performance of CT in this application was limited, primarily by size criteria: nodes >10 mm in the smallest diameter are suspected of involvement by NSCLC. The limitations of this size-based nodal characterization are well documented, as up to 21% of nodes <10 mm are malignant, whereas 40% of nodes >10 mm are benign (14,15). In the present study, PET-CT was characterized by a 95.8% negative predictive value in the detection of regional LNs. These data conformed with the results of previous studies, which demonstrated negative predictive values of up to 94-96% (14,15). As was demonstrated by Antoch *et al* (14), a diagnosis of N0 disease with PET-CT does not require additional verification with mediastinal lymph node mapping. Although the positive predictive value of PET-CT (86.5%) was higher compared to that of contrast-enhanced CT (60.6%), the differentiation between malignancy and increased glucose metabolism caused by an inflammatory lymph node reaction remains challenging. In certain cases, benign conditions, such as inflammatory lesions, may also display a higher radioactivity uptake and the value of SUVmax may exceed 2.5; however, the combination of CT findings, e.g., morphological characteristics, density, distribution with delayed-phase PET findings, e.g., changes in the degree of radioactive uptake, may be helpful in differentiating between malignant and benign lesions, as was reported by our center (16).

In the present study, comparisons were conducted between different histological subtypes for MTV and SUVmax. The results revealed an association between metabolic parameters and the histopathology of the primary tumor, as the SUVmax and MTV were significantly higher in SCC compared to those in AC. This observation is in line with the results of previous studies (17,18). It was previously reported that a higher FDG uptake correlates with more rapid lung cancer cell proliferation and a reduced tumor doubling time (19). Furthermore, the tumor volume is also an important factor contributing to FDG uptake. The present study also demonstrated a correlation

between the MTV of the primary tumor and the degree of FDG accumulation (SUVmax) in both AC and SCC. These findings may partly explain the higher SUVmax in SCC compared to AC patients in our study.

In addition, the uptake of FDG in the primary tumor reflects some biological information, including proliferative activity (20), tumor doubling time (21), microvessel density (22), histological subtype (17,18) and tumor grading (17). In the present study, the FDG uptake and MTV of the primary tumor were significantly different among subgroups by differentiation in both AC and SCC. This finding is consistent with the hypothesis that the glucose metabolism measured by FDG-PET may vary proportionately with the proliferative activity of the tumor cells, which, in turn, is known to correlate with tumor aggressiveness. All these findings may contribute to the association between FDG uptake, biological aggressiveness and prognosis in NSCLC cases.

There were several limitations to the present study, including the retrospective nature of the study design, the relatively low number of patients in our cohort and the heterogeneity of the patients and treatments. In particular, SUV 2.5 was used to define the contouring margins around the target lesions as a fixed threshold. Nonetheless, SUV may be affected by several factors (23,24) and we acknowledge that the optimal threshold may vary depending on the PET center and tumor characteristics. Therefore, we aim to continue our study to enroll more patients, as confirmation as well as for future subgroup analysis.

In conclusion, the effect of PET-CT on clinical staging of NSCLC was significant. Whole-body ^{18}F-FDG PET-CT appears to be a precise, highly efficient and non-invasive method for T and N staging in patients with NSCLC, due to its higher sensitivity, specificity and accuracy compared to contrast-enhanced CT, the most widely used method for staging evaluation. Therefore, ^{18}F-FDG PET-CT is an important compensatory staging measure. The FDG uptake of the primary tumor was associated with histological type and differentiation and the differences were statistically significant. Therefore, the SUVmax and MTV of the primary tumor may be valuable indices to partly predict the histological type and the grade of differentiation of NSCLC.

References

1. Antoch G, Saoudi N, Kuehl H, *et al*: Accuracy of whole-body dual-modality fluorine-18-2-fluoro-2-deoxy-D-glucose positron emission tomography and computed tomography (FDG-PET/CT) for tumor staging in solid tumors: comparison with CT and PET. J Clin Oncol 22: 4357-4368, 2004.
2. MacDonald K, Searle J and Lyburn I: The role of dual time point FDG PET imaging in the evaluation of solitary pulmonary nodules with an initial standard uptake value less than 2.5. Clin Radiol 66: 244-250, 2011.
3. Shum WY, Hsieh TC, Yeh JJ, *et al*: Clinical usefulness of dual-time FDG PET-CT in assessment of esophageal squamous cell carcinoma. Eur J Radiol 81: 1024-1028, 2012.
4. Xiu Y, Bhutani C, Dhurairaj T, *et al*: Dual-time point FDG PET imaging in the evaluation of pulmonary nodules with minimally increased metabolic activity. Clin Nucl Med 32: 101-105, 2007.
5. Hu Q, Wang W, Zhong X, *et al*: Dual-time-point FDG PET for the evaluation of locoregional lymph nodes in thoracic esophageal squamous cell cancer. Eur J Radiol 70: 320-324, 2009.
6. Hong R, Halama J, Bova D, Sethi A and Emami B: Correlation of PET standard uptake value and CT window-level thresholds for target delineation in CT-based radiation treatment planning. Int J Radiat Oncol Biol Phys 67: 720-726, 2007.
7. Leong T, Everitt C, Yuen K, *et al*: A prospective study to evaluate the impact of FDG-PET on CT-based radiotherapy treatment planning for oesophageal cancer. Radiother Oncol 78: 254-261, 2006.
8. Zhu D, Ma T, Niu Z, *et al*: Prognostic significance of metabolic parameters measured by ^{18}F-fluorodeoxyglucose positron emission tomography/computed tomography in patients with small cell lung cancer. Lung Cancer 73: 332-337, 2011.
9. Naruke T, Suemasu K and Ishikawa S: Surgical treatment for lung cancer with metastasis to mediastinal lymph nodes. J Thorac Cardiovasc Surg 71: 279-285, 1976.
10. Martini N and Flehinger BJ: The role of surgery in N2 lung cancer. Surg Clin North Am 67: 1037-1049, 1987.
11. Izbicki JR, Thetter O, Habekost M, *et al*: Radical systematic mediastinal lymphadenectomy in non-small cell lung cancer: a randomized controlled trial. Br J Surg 81: 229-235, 1994.
12. Tsim S, O'Dowd CA, Milroy R and Davidson S: Staging of non-small cell lung cancer (NSCLC): a review. Respir Med 104: 1767-1774, 2010.
13. Wrona A and Jassem J: The new TNM classification in lung cancer. Pneumonol Alergol Pol 78: 407-417, 2010 (In Polish).
14. Antoch G, Stattaus J, Nemat AT, *et al*: Non-small cell lung cancer: dual-modality PET/CT in preoperative staging. Radiology 229: 526-533, 2003.
15. Dwamena BA, Sonnad SS, Angobaldo JO and Wahl RL: Metastases from non-small cell lung cancer: mediastinal staging in the 1990s--meta-analytic comparison of PET and CT. Radiology 213: 530-536, 1999.
16. Hu M, Han A, Xing L, *et al*: Value of dual-time-point FDG PET/CT for mediastinal nodal staging in non-small-cell lung cancer patients with lung comorbidity. Clin Nucl Med 36: 429-433, 2011.
17. de Geus-Oei LF, van Krieken JH, Aliredjo RP, *et al*: Biological correlates of FDG uptake in non-small cell lung cancer. Lung Cancer 55: 79-87, 2007.
18. Li M, Liu N, Hu M, *et al*: Relationship between primary tumor fluorodeoxyglucose uptake and nodal or distant metastases at presentation in T1 stage non-small cell lung cancer. Lung Cancer 63: 383-386, 2009.
19. Higashi K, Ueda Y, Yagishita M, *et al*: FDG PET measurement of the proliferative potential of non-small cell lung cancer. J Nucl Med 41: 85-92, 2000.
20. Higashi K, Ueda Y, Ayabe K, *et al*: FDG PET in the evaluation of the aggressiveness of pulmonary adenocarcinoma: correlation with histopathological features. Nucl Med Commun 21: 707-714, 2000.
21. Duhaylongsod FG, Lowe VJ, Patz EF Jr, Vaughn AL, Coleman RE and Wolfe WG: Lung tumor growth correlates with glucose metabolism measured by fluoride-18 fluorodeoxyglucose positron emission tomography. Ann Thorac Surg 60: 1348-1352, 1995.
22. Guo J, Higashi K, Ueda Y, *et al*: Microvessel density: correlation with ^{18}F-FDG uptake and prognostic impact in lung adenocarcinomas. J Nucl Med 47: 419-425, 2006.
23. Boellaard R, Krak NC, Hoekstra OS and Lammertsma AA: Effects of noise, image resolution, and ROI definition on the accuracy of standard uptake values: a simulation study. J Nucl Med 45: 1519-1527, 2004.
24. Westerterp M, Pruim J, Oyen W, *et al*: Quantification of FDG PET studies using standardised uptake values in multi-centre trials: effects of image reconstruction, resolution and ROI definition parameters. Eur J Nucl Med Mol Imaging 34: 392-404, 2007.